



ORIGINAL ARTICLE

Design and synthesis of novel indole-quinoxaline hybrids to target phosphodiesterase 4 (PDE4)



Bethala Jawahar Luther^a, Chekuri Sharmila Rani^b, Namburi Suresh^b,
Mandava V. Basaveswara Rao^{b,*}, Ravikumar Kapavarapu^c, Chakali Suresh^d,
P. Vijaya Babu^d, Manojit Pal^{d,*}

^a Department of Chemistry, Acharya Nagarjuna University, Guntur, Andhra Pradesh, India

^b Department of Chemistry, Krishna University, Krishna Dist., Andhra Pradesh, India

^c Doctoral Programme in Experimental Biology and Biomedicine, Center for Neuroscience and Cell Biology, University of Coimbra, 3004-517 Coimbra, Portugal

^d Dr. Reddy's Institute of Life Sciences, University of Hyderabad Campus, Hyderabad 500046, India

Received 28 May 2015; accepted 6 August 2015

Available online 13 August 2015

KEYWORDS

Indole;
Quinoxaline;
Pd/C;
PDE4

Abstract A series of novel hybrid molecules were designed rationally by connecting an indole moiety with a quinoxaline ring through a linker as potential inhibitors of PDE4. Their design was validated initially *in silico* by performing docking studies using a representative molecule. Subsequent synthesis of a focused library of related hybrid molecules was accomplished using Pd/C—Cu mediated coupling-cyclization as a key step. Some of the synthesized compounds showed PDE4 inhibition *in vitro* and one of them appeared to be promising.

© 2015 The Authors. Published by Elsevier B.V. on behalf of King Saud University. This is an open access article under the CC BY-NC-ND license (<http://creativecommons.org/licenses/by-nc-nd/4.0/>).

1. Introduction

Design of small organic molecules via incorporation of two or more ‘privileged scaffolds’ into a single molecular entity has been a useful approach for identification of novel and efficient ligands for various biological targets (Evans et al., 1988). While

considerable efforts have been devoted on application of privileged structures in drug design and discovery (DeSimone et al., 2004; Welsch et al., 2010) only a handful number of reports are known on exploring the strategy of incorporating two or more ‘privileged scaffolds’ in a single molecule. For example, an indolyl-quinoxaline (Fig. 1) where two heterocycles were connected through the indole N – 1 nitrogen was explored as a PAS kinase-inhibitor (McCall et al., 2011). Notably, being present in a diverse range of drugs and natural products with associated pharmacological activity indoles and quinoxalines are considered as ‘privileged scaffolds’ and are of significant importance in the drug development arena. This encouraged us to focus on some novel indole-quinoxaline hybrids to target phosphodiesterase 4 (PDE4).

* Corresponding author. Tel.: +91 40 6657 1500.

E-mail addresses: vbrmandava@yahoo.com (M.V. Basaveswara Rao), manojitpal@rediffmail.com (M. Pal).

Peer review under responsibility of King Saud University.



Production and hosting by Elsevier

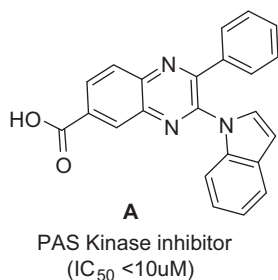


Figure 1 Example of indolyl-quinoxaline as a PAS kinase inhibitor.

The enzyme phosphodiesterase 4 (PDE4), one of the 11 families of PDEs (PDE1-PDE11) has emerged as a promising pharmacological target for the potential treatment of COPD and asthma, a major public health burden worldwide. While several selective PDE4 inhibitors (Kodimuthali et al., 2008) have been developed as potential drugs including the recently marketed roflumilast for the treatment of both COPD and asthma, their launching has been delayed due to the undesired side effects especially emesis (Spina, 2008; Rabe, 2011; Lipworth, 2005). While the mechanisms for the side effects observed with PDE4-selective inhibitors are not clearly understood one of the approaches to overcome this problem is to design, synthesize and evaluate new class of molecules for their potential as PDE4 inhibitors. Though the use of strategy based on hybrid molecule for the discovery of new drugs is noteworthy in the area of anticancer and antimalarial research (Chauhan et al., 2010), its use is not common in the identification of new PDE4 inhibitors. Nevertheless, the structural features of an indole based potent PDE4 inhibitor (Gutke et al., 2005; Draheim et al., 2004; Tralau-Stewart et al., 2011) AWD-12-281 (Fig. 2) and our interest in quinoxaline derivatives (Kumar et al., 2012a, 2012b; Nakhi et al., 2013a, 2013b; Babu et al., 2013; Sunke et al., 2014; Kolli et al., 2014a, 2014b) prompted us to explore the strategy of hybrid molecules for the identification of new PDE4 inhibitors. Thus a new template **A** (Fig. 2) was designed by connecting the indole moiety with the quinoxaline ring through a linker to generate a library of hybrid molecules for testing against PDE4. Herein, we report our preliminary results of this study. Compounds represented by **A** (i.e. **6**) were synthesized according to the procedure shown in Scheme 1.

2. Materials and methods

2.1. General

Unless otherwise stated, reactions were performed under nitrogen atmosphere using oven dried glassware. Reactions were monitored by thin layer chromatography (TLC) on silica gel plates (60 F254), visualized with ultraviolet light or iodine spray. Flash chromatography was performed on silica gel (230–400 mesh) using distilled hexane, ethyl acetate, and dichloromethane. NMR spectra were determined in CDCl₃ solution by using a 400 MHz spectrometer. Proton chemical shifts (δ) are relative to tetramethylsilane (TMS, $\delta = 0.00$) as internal standard and expressed in ppm. Spin multiplicities are given as s (singlet), d (doublet), t (triplet) and m (multiplet)

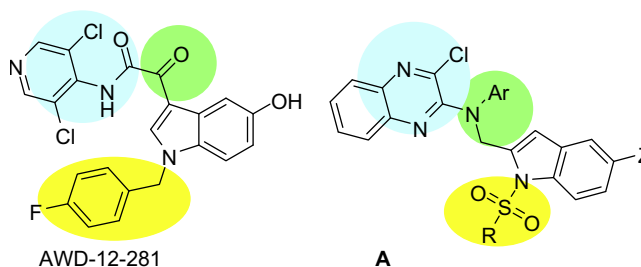


Figure 2 Known PDE4 inhibitor AWD-12-281 and the design of potential PDE4 inhibitor **A/B**.

as well as bm (broad multiplet). Coupling constants (J) are given in hertz. Infrared spectra were recorded on a FT-IR spectrometer. MS spectra were obtained on a mass spectrometer (Agilent 6430 Triple Quadrupole LC/MS).

2.2. Synthesis of compound 4

A mixture of compound **3** (1.0 mmol), propargyl bromide (1.5 mmol) and NaH (1.5 eq) in THF (5 mL) was stirred at room temp for 2–4 h under a nitrogen atmosphere. After completion of the reaction (TLC), the mixture was poured into ice-cold water (15 mL), stirred for 10 min and then extracted with ethyl acetate (3 × 10 mL). The organic layers were collected, combined, washed with cold water (2 × 10 mL), dried over anhydrous Na₂SO₄, filtered and concentrated under low vacuum. The residue obtained was purified by column chromatography on silica gel (230–400 mesh) using ethyl acetate/hexane to give the desired product.

2.3. 3-Chloro-*N*-(4-chlorophenyl)-*N*-(prop-2-ynyl)quinoxalin-2-amine (**4a**)

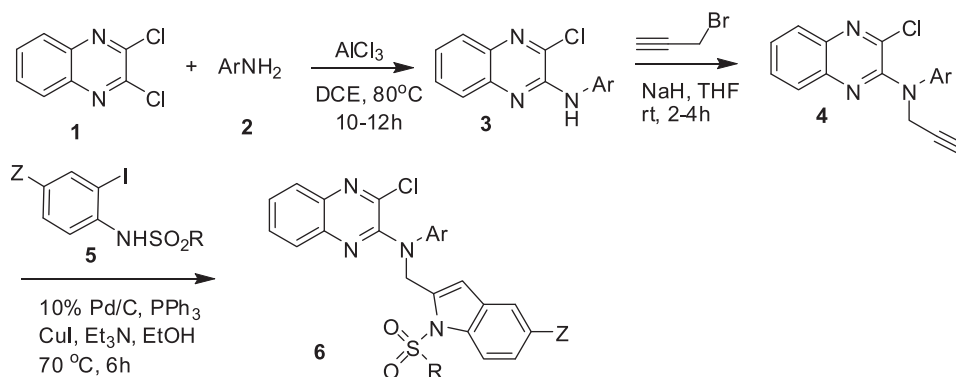
IR (KBr, cm⁻¹): 3275.3 (\equiv C–H), 2105.5 ($\text{--C}\equiv\text{C--}$), 1541.6, 1490.3, 1362.3, 1225.9, 1073.2; ¹H NMR (400 MHz, CDCl₃) δ : 7.94 (dd, $J = 8.4, 0.9$ Hz, 1H), 7.91 (dd, $J = 8.3, 1.2$ Hz, 1H), 7.73–7.68 (m, 1H), 7.62–7.57 (m, 1H), 7.36–7.31 (m, 2H), 7.09–7.04 (m, 2H), 4.74 (d, $J = 2.4$ Hz, 2H, CH₂), 2.21 (t, $J = 2.4$ Hz, 1H, \equiv CH); MS (ES mass): 328.0 (M + 1).

2.4. 3-Chloro-*N*-(4-fluorophenyl)-*N*-(prop-2-ynyl)quinoxalin-2-amine (**4b**)

IR (KBr, cm⁻¹): 3274.4 (\equiv C–H), 2108.3 ($\text{--C}\equiv\text{C--}$), 1535.1, 1486.8, 1334.3, 1218.9, 1072.9; ¹H NMR (400 MHz, CDCl₃) δ : 7.94 (d, $J = 8.4$ Hz, 1H), 7.90 (d, $J = 8.0$ Hz, 1H), 7.71–7.67 (m, 1H), 7.60–7.56 (m, 1H), 7.14–7.11 (m, 2H), 7.08–7.04 (m, 2H), 4.71 (d, $J = 2.3$ Hz, 2H, CH₂), 2.21 (t, $J = 2.3$ Hz, 1H, \equiv CH); MS (ES mass): 311.8 (M + 1).

2.5. Synthesis of compound 6

A mixture of compound **4** (1.2 mmol), 10% Pd/C (0.02 mmol), PPh₃ (0.15 mmol), CuI (0.03 mmol), and triethylamine (2.40 mmol) in ethanol (5 mL) was stirred at 25–30 °C for 30 min under nitrogen. To this was added *o*-iodoaniline (**5**) (1.2 mmol), and the mixture was initially stirred at room temperature for 1 h and then at 70 °C for 6 h. After completion of



Scheme 1 Synthesis of quinoxaline-indole based hybrid molecules **6**.

the reaction, the mixture was cooled to room temperature, diluted with EtOAc (50 mL), and filtered through Celite. The organic layers were collected, combined, washed with water (3 × 30 mL), dried over anhydrous Na₂SO₄, filtered and concentrated under low vacuum. The crude residue was purified by column chromatography on silica gel using methanol/dichloromethane to afford the desired product.

2.6. 3-Chloro-N-(4-chlorophenyl)-N-((1-(methylsulfonyl)-1H-indol-2-yl)methyl)quinoxalin-2-amine (6a)

¹H NMR (400 MHz, CDCl₃) δ 8.04 (d, *J* = 8.2 Hz, 1H, C-8 quinoxaliny H), 7.95 (d, *J* = 7.8 Hz, 1H, C-5 quinoxaliny H), 7.77 (d, *J* = 8.3 Hz, 1H, C-7 indolyl H), 7.68–7.67 (m, 1H, quinoxaliny H), 7.63–7.62 (m, 1H, quinoxaliny H), 7.48 (d, *J* = 7.6 Hz, 1H, C-4 indolyl H), 7.37–7.29 (m, 2H, C-5 & C-6 indolyl H), 7.27 (d, *J* = 8.6 Hz, 2H, ArH), 7.02 (d, *J* = 8.6 Hz, 2H, ArH), 6.79 (s, 1H, C-3 indolyl H), 5.66 (s, 2H, CH₂), 3.29 (s, 3H, MeSO₂); ¹³C NMR (100 MHz, CDCl₃) δ ppm 148.9 (C-2 quinoxaliny), 145.6 (C-1 4-chlorophenyl), 142.2 (C-3 quinoxaliny), 139.7 (C-2 indolyl), 138.9, 137.7, 137.0, 130.6, 130.5, 129.6 (2C), 129.1, 128.2, 127.8, 126.7, 124.6, 124.0 (2C), 123.8, 120.8, 113.8, 109.9 (C-3 indolyl), 51.9 (—CH₂—), 40.9 (—CH₃SO₂—); MS (ES mass): 497.1 (M + 1); HPLC: 97.2%, column: X Terra C-18 250 × 4.6 mm 5 μm, mobile phase A: 5% ammonium acetate in water, mobile phase B: CH₃CN, gradient (T/%B): 0/20, 3/20, 12/95, 23/95, 25/20, 30/20; flow rate: 1.0 mL/min; UV 210 nm.

2.7. 3-Chloro-N-(4-chlorophenyl)-N-((5-methyl-1-(methylsulfonyl)-1H-indol-2-yl)methyl)quinoxalin-2-amine (6b)

¹H NMR (400 MHz, CDCl₃) δ 7.89–7.87 (m, 2H), 7.72 (d, *J* = 8.6 Hz, 1H), 7.67–7.63 (m, 1H), 7.60–7.55 (m, 1H), 7.59 (m, 1H), 7.27 (d, *J* = 8.6 Hz, 2H), 7.02 (d, *J* = 8.6 Hz, 2H), 7.14–7.09 (m, 1H), 6.68 (s, 1H, C-3 indolyl H), 5.57 (s, 2H, CH₂), 3.29 (s, 3H, MeSO₂), 2.39 (s, 3H, CH₃); MS (ES mass): 511.3 (M + 1); HPLC: 97.6%, column: X Bridge C-18 150 × 4.6 mm 5 μm, mobile phase A: 0.1% HCOOH in water, mobile phase B: CH₃CN, gradient (T/%B): 0/40, 2/40, 9/98, 16/98, 17/40, 20/40; flow rate: 1.0 mL/min; UV 215 nm.

2.8. 3-Chloro-N-(4-chlorophenyl)-N-((5-methoxy-1-(methylsulfonyl)-1H-indol-2-yl)methyl)quinoxalin-2-amine (6c)

¹H NMR (400 MHz, CDCl₃) δ 7.88–7.86 (m, 1H), 7.71 (d, *J* = 8.6 Hz, 1H), 7.66–7.63 (m, 1H), 7.60–7.56 (m, 2H), 7.23 (s, 1H), 7.27 (d, *J* = 8.6 Hz, 2H), 7.13–7.08 (m, 1H), 7.02 (d, *J* = 8.6 Hz, 2H), 6.67 (s, 1H, C-3 indolyl H), 5.56 (s, 2H, CH₂), 3.89 (s, 3H, OCH₃), 3.24 (s, 3H, MeSO₂); MS (ES mass): 527.2 (M + 1); HPLC: 96.8%, column: X Bridge C-18 150 × 4.6 mm 5 μm, mobile phase A: 0.1% HCOOH in water, mobile phase B: CH₃CN, gradient (T/%B): 0/40, 2/40, 9/98, 16/98, 17/40, 20/40; flow rate: 1.0 mL/min; UV 215 nm.

2.9. 3-Chloro-N-(4-fluorophenyl)-N-((1-(methylsulfonyl)-1H-indol-2-yl)methyl)quinoxalin-2-amine (6d)

¹H NMR (400 MHz, CDCl₃) δ 7.92–7.90 (m, 1H), 7.79 (d, *J* = 8.6 Hz, 1H), 7.75 (d, *J* = 8.3 Hz, 1H), 7.67–7.63 (m, 1H), 7.60–7.55 (m, 1H), 7.48 (d, *J* = 7.6 Hz, 1H), 7.37–7.29 (m, 2H), 7.06–6.98 (m, 4H), 6.78 (s, 1H, C-3 indolyl H), 5.62 (s, 2H, CH₂), 3.24 (s, 3H, MeSO₂); MS (ES mass): 480.9 (M + 1); HPLC: 96.9%, column: X Bridge C-18 150 × 4.6 mm 5 μm, mobile phase A: 0.1% HCOOH in water, mobile phase B: CH₃CN, gradient (T/%B): 0/40, 2/40, 9/98, 16/98, 17/40, 20/40; flow rate: 1.0 mL/min; UV 215 nm.

2.10. 3-Chloro-N-(4-fluorophenyl)-N-((5-methyl-1-(methylsulfonyl)-1H-indol-2-yl)methyl)quinoxalin-2-amine (6e)

¹H NMR (400 MHz, CDCl₃) δ 7.89 (m, 2H, C-8 quinoxaliny H + C-7 indolyl H), 7.72 (d, *J* = 8.6 Hz, 1H, C-5 quinoxaliny H), 7.67–7.63 (m, 1H, quinoxaliny H), 7.60–7.55 (m, 1H, quinoxaliny H), 7.24 (s, 1H, C-4 indolyl H), 7.14–7.09 (m, 1H, C-6 indolyl H), 7.07–6.99 (m, 4H, ArH), 6.68 (s, 1H, C-3 indolyl H), 5.58 (s, 2H, CH₂), 3.25 (s, 3H, MeSO₂), 2.39 (s, 3H, Me); MS (ES mass): 494.8 (M + 1); HPLC: 96.8%, column: X Bridge C-18 150 × 4.6 mm 5 μm, mobile phase A: 0.1% HCOOH in water, mobile phase B: CH₃CN, gradient (T/%B): 0/40, 2/40, 9/98, 16/98, 17/40, 20/40; flow rate: 1.0 mL/min; UV 215 nm.

2.11. 3-Chloro-N-(4-fluorophenyl)-N-((5-methoxy-1-(methylsulfonyl)-1H-indol-2-yl)methyl)quinoxalin-2-amine (6f)

¹H NMR (400 MHz, CDCl₃) δ 7.88–7.86 (m, 1H), 7.71 (d, *J* = 8.6 Hz, 1H), 7.66–7.63 (m, 1H), 7.60–7.56 (m, 2H), 7.23 (s, 1H), 7.13–7.08 (m, 1H), 7.06–6.98 (m, 4H), 6.67 (s, 1H), 5.56 (s, 2H, CH₂), 3.89 (s, 3H, OCH₃), 3.24 (s, 3H); MS (ES mass): 510.97 (M + 1); HPLC: 98.1%, column: X Bridge C-18 150 × 4.6 mm 5 μm, mobile phase A: 0.1% HCOOH in water, mobile phase B: CH₃CN, gradient (T/%B): 0/40, 2/40, 9/98, 16/98, 17/40, 20/40; flow rate: 1.0 mL/min; UV 215 nm.

2.12. 3-Chloro-N-(4-fluorophenyl)-N-((1-tosyl-1H-indol-2-yl)methyl)quinoxalin-2-amine (6g)

¹H NMR (400 MHz, CDCl₃) δ 8.03 (dd, *J* = 9.1, 4.2 Hz, 1H), 7.91 (d, *J* = 8.0 Hz, 1H), 7.76 (d, *J* = 8.3 Hz, 3H), 7.67 (m, 2H), 7.48 (d, *J* = 7.6 Hz, 1H), 7.37–7.29 (m, 2H), 7.24 (d, *J* = 8.1 Hz, 2H), 7.04–6.95 (m, 4H), 6.74 (s, 1H), 5.68 (s, 2H), 2.39 (s, 3H); MS (ES mass): 557.02 (M + 1); HPLC: 98.2%, column: X Bridge C-18 150 × 4.6 mm 5 μm, mobile phase A: 0.1% HCOOH in water, mobile phase B: CH₃CN, gradient (T/%B): 0/40, 2/40, 9/98, 16/98, 17/40, 20/40; flow rate: 1.0 mL/min; UV 215 nm.

2.13. 3-Chloro-N-((5-fluoro-1-tosyl-1H-indol-2-yl)methyl)-N-(4-fluorophenyl)quinoxalin-2-amine (6h)

¹H NMR (400 MHz, CDCl₃) δ 8.05 (dd, *J* = 9.1, 4.2 Hz, 1H, C-8 quinoxaliny H), 7.92 (d, *J* = 8.0 Hz, 1H, C-5 quinoxaliny H), 7.77 (d, *J* = 8.3 Hz, 2H, ArH), 7.67 (m, 2H, quinoxaliny H), 7.59 (m, 1H, C-4 indolyl H), 7.24 (d, *J* = 8.1 Hz, 2H, ArH), 7.04–6.95 (m, 6H, ArH + indolyl H), 6.64 (s, 1H, C-3 indolyl H), 5.76 (s, 2H, CH₂), 2.39 (s, 3H, Me); MS (ES mass): 574.8 (M + 1); HPLC: 97.5%, column: X Bridge C-18 150 × 4.6 mm 5 μm, mobile phase A: 0.1% HCOOH in water, mobile phase B: CH₃CN, gradient (T/%B): 0/40, 2/40, 9/98, 16/98, 17/40, 20/40; flow rate: 1.0 mL/min; UV 215 nm.

2.14. 3-Chloro-N-(4-fluorophenyl)-N-((5-methyl-1-tosyl-1H-indol-2-yl)methyl)quinoxalin-2-amine (6i)

¹H NMR (400 MHz, CDCl₃) δ 7.89–7.87 (m, 2H), 7.72 (d, *J* = 8.6 Hz, 1H), 7.77 (d, *J* = 8.3 Hz, 2H), 7.67–7.63 (m, 1H), 7.60–7.55 (m, 1H), 7.59 (m, 1H), 7.24 (d, *J* = 8.1 Hz, 2H), 7.14–7.09 (m, 1H), 7.07–6.99 (m, 4H), 6.68 (s, 1H, C-3 indolyl H), 5.58 (s, 2H, CH₂), 2.40 (s, 3H, CH₃), 2.39 (s, 3H, CH₃); MS (ES mass): 571.09 (M + 1); HPLC: 97.3%, column: X Bridge C-18 150 × 4.6 mm 5 μm, mobile phase A: 0.1% HCOOH in water, mobile phase B: CH₃CN, gradient (T/%B): 0/40, 2/40, 9/98, 16/98, 17/40, 20/40; flow rate: 1.0 mL/min; UV 215 nm.

2.15. Docking procedure

The PDE4B receptor in complex with Rolipram (PDB code-IXMY) was used as the receptor for docking study. The original PDB file contains crystallized Zn and Mg metal ions. The PDE Proteins were retrieved from PDB and

Protonated (addition of Hydrogen atoms) with Protonation 3D application in MOE, Connolly Molecular surface was generated around the ligand site of the protein, and Gasteiger Partial charges were added to the protein and finally energy minimized to relieve bad crystallographic contacts. “Active site finder” function of the MOE software was used to denote potential docking pockets within the Protein crystal structure. The test compounds were placed in the Active site pocket of the protein by the “Triangle Matcher” method, which generated poses by aligning the ligand triplet of atoms with the triplet of alpha spheres in cavities of tight atomic packing. Dock scoring was carried out using the London dG method and then retaining and scoring the best 10 poses of molecules finally. The preparation of the ligands for Docking Simulation involved the energy minimization with Molecular Mechanics Force-field MMFF94x (Merck Molecular Force Field 94x) and then molecules were subjected to conformational search in MOE using the Conformations Stochastic search module to find the lowest energy conformers.

The docking results were appeared as Docking Score in which the docking poses were ranked by the Molecular Mechanics and Generalized Born solvation model (MM/GBVI) binding free energy.

For all scoring functions, lower scores indicated more favorable poses. The unit for all scoring functions is kcal/mol. The final energy was calculated using the Generalized Born solvation model. Poses for each ligand were scored based on complementarity with the binding pocket.

The London dG scoring function estimated the free energy of binding of the ligand from a given pose. The functional form is a sum of terms:

$$\Delta G = c + E_{flex} + \sum_{h-bonds} c_{HB} f_{HB} + \sum_{m-lig} c_M f_M + \sum_{atoms\ i} \Delta D_i$$

where *c* represents the average gain/loss of rotational and translational entropy; *E_{flex}* is the energy due to the loss of flexibility of the ligand (calculated from ligand topology only); *f_{HB}* measures geometric imperfections of hydrogen bonds and takes a value in [0,1]; *c_{HB}* is the energy of an ideal hydrogen bond; *f_M* measures geometric imperfections of metal ligations and takes a value in [0,1]; *c_M* is the energy of an ideal metal ligation; and *D_i* is the desolvation energy of atom *i*.

2.16. In vitro assay for PDE4B

2.16.1. Cells and reagents

Sf9 cells were obtained from ATCC (Washington, DC, USA) and were routinely maintained in Grace's supplemented medium (Invitrogen) with 10% FBS. cAMP was purchased from SISCO Research Laboratories (Mumbai, India). PDElight HTS cAMP phosphodiesterase assay kit was procured from Lonza (Basel, Switzerland). PDE4B1 clone was procured from OriGene Technologies (Rockville, MD, USA). PDE4D2 enzyme was purchased from BPS Bioscience (San Diego, CA, USA).

2.16.2. PDE4B protein production and purification

PDE4B1 cDNA was sub-cloned into pFAST Bac HTB vector (Invitrogen) and transformed into DH10Bac (Invitrogen) competent cells. Recombinant bacmids were tested for integration by PCR analysis. Sf9 cells were transfected with bacmid using

Lipofectamine 2000 (Invitrogen) according to manufacturer's instructions. Subsequently, P3 viral titer was amplified, cells were infected and 48 h postinfection cells were lysed in lysis buffer (50 mM Tris-HCl pH 8.5, 10 mM 2-Mercaptoethanol, 1% protease inhibitor cocktail (Roche), 1% NP40). Recombinant His-tagged PDE4B protein was purified as previously described elsewhere (Wang et al., 1997). Briefly, lysate was centrifuged at 10,000 rpm for 10 min at 4 °C and supernatant was collected. Supernatant was mixed with Ni-NTA resin (GE Life Sciences) in a ratio of 4:1 (v/v) and equilibrated with binding buffer (20 mM Tris-HCl pH 8.0, 500 mM-KCl, 5 mM imidazole, 10 mM 2-mercaptoethanol and 10% glycerol) in a ratio of 2:1 (v/v) and mixed gently on rotary shaker for 1 h at 4 °C. After incubation, lysate-Ni-NTA mixture was centrifuged at 4500 rpm for 5 min at 4 °C and the supernatant was collected as the flow-through fraction. Resin was washed twice with wash buffer (20 mM Tris-HCl pH 8.5, 1 M KCl, 10 mM 2-Mercaptoethanol and 10% glycerol). Protein was eluted sequentially twice using elution buffers (Buffer I: 20 mM Tris-HCl pH 8.5, 100 mM KCl, 250 mM imidazole, 10 mM 2-mercaptoethanol, 10% glycerol, Buffer II: 20 mM Tris-HCl pH 8.5, 100 mM KCl, 500 mM imidazole, 10 mM 2-mercaptoethanol, 10% glycerol). Eluates were collected in four fractions and analyzed by SDS-PAGE. Eluates containing PDE4B protein were pooled and stored at -80 °C in 50% glycerol until further use.

2.16.3. PDE4 enzymatic assay

The inhibition of PDE4 enzyme was measured using PDE light HTS cAMP phosphodiesterase assay kit (Lonza) according to manufacturer's recommendations. Briefly, 10 ng of in house purified PDE4B1 enzyme was pre-incubated either with DMSO (vehicle control) or with compound for 15 min before incubation with the substrate cAMP (5 μM) for 1 h. The reaction was halted with stop solution and reaction mix was incubated with detection reagent for 10 min in dark. Luminescence values (RLUs) were measured by a Multilabel plate reader (Perkin Elmer 1420 Multilabel counter). The percentage of inhibition was calculated using the following formula:

$$\% \text{inhibition} = \frac{(\text{RLU of vehicle control} - \text{RLU of inhibitor})}{\text{RLU of vehicle control}} \times 100$$

3. Results and discussion

3.1. Docking studies

Before undertaking the actual chemical synthesis of the library of hybrid molecules based on **A**, we performed *in silico* docking studies (Card et al., 2004; Corbeil et al., 2012; Dym et al., 2002; Oliveria et al., 2006; Gangwal et al., 2015; França et al., 2013) using a specific molecule **B** (Fig. 3) that belongs to **A**. We also used the individual fragment of **B** e.g. **C** and **D** (Fig. 3) for the docking studies to assess the usefulness of our concept in the present case. It is known that the PDE4 enzyme has four subtypes e.g. PDE4A, B, C, and D of which PDE4B is the major subtype responsible for mediating LPS-induced inflammation (Kodimuthali et al., 2008). Thus apart from cyclooxygenase-2 inhibition (Ramalho et al., 2009), the inhibition of PDE4B has been hypothesized as the basis of effective

anti-inflammatory treatment and therefore this particular subtype was chosen as the target protein for both *in silico* and *in vitro* studies. A well known PDE4 inhibitor rolipram (Fig. 3) was used as a reference compound in these studies.

The molecular docking simulation studies were performed using the Chemical Computing Group's Molecular Operating Environment (MOE) software 2008.10 Version, "DOCK" application module. The PDE4B receptor in complex with rolipram (PDB code-1XMY) was used as the receptor for docking. To validate the docking accuracy of the program used, the native co-crystallized rolipram ligand was docked back into its binding site of PDE4B protein. The molecule **B** and its two individual fragments **C** and **D** along with the reference compound rolipram were docked into the PDE4B protein. The docking studies mainly involved searching for favorable binding configurations of ligands in macromolecular target (i.e. the PDE4B protein) and for each ligand, a number of configurations called *poses* were generated and scored in an effort to determine favorable binding modes. The results are summarized in Table 1.

It is evident from Table 1 that the molecule **B** showed dock score comparable with rolipram whereas dock score of its individual fragments **C** and **D** was found to be inferior. In view of the fact that dock score is the reflection of extent of binding of a given molecule with the target protein, **C** and **D** appeared as mediocre inhibitors of PDE4B *in silico*. However, their combined form **B** was identified as a better and potential inhibitor of PDE4B indicating usefulness of the concept. The docking studies also demonstrated that these compounds utilized the conserved binding site of the PDE4B protein whereby the sulphonyl oxygen of the indole ring played a major role in forming H-bond. In general, these compounds interacted either with the conserved residues such as Tyr233 of Q pocket (e.g. compounds **C** and **D**, see supporting info) or with His234 of metal binding pocket (e.g. compound **B**) in the active site of PDE4B and most of them showed a common arene-arene interaction with Phe446. The docking of compound **B** is shown in Fig. 4. Notably, like **B** rolipram also formed H-bond with His234 of PDE4B.

3.2. Chemistry

In view of the promising *in silico* results obtained for **B** through docking studies we planned to synthesize molecules based on **A** including **B**. A Pd/C-catalyzed coupling-cyclization strategy leading to the formation of indole ring was used to prepare our target molecules (Scheme 1) (Pal, 2009; Pal et al., 2004; Layek et al., 2009). We preferred this strategy as the concerned methodology involved the use of less expensive, stable, easy to handle and recyclable Pd/C which is advantageous over the other Pd-based methodologies. Moreover, this strategy is known to allow the construction of appropriately substituted indole ring of our choice. The starting alkyne (**4**) was prepared *via* propargylation of *N*-aryl substituted 3-chloroquinoxalin-2-amine (**3**) which in turn was prepared *via* the reaction of 2,3-dichloroquinoxaline (**1**) with anilines (**2**) in the presence of AlCl₃ in 1,2-dichloroethane (DCE) (Prasad et al., 2012). The terminal alkyne **4** thus obtained was used for the coupling-cyclization with a range of *o*-iodoanilides (**5**) in the presence of 10% Pd/C, PPh₃, CuI and Et₃N in EtOH.

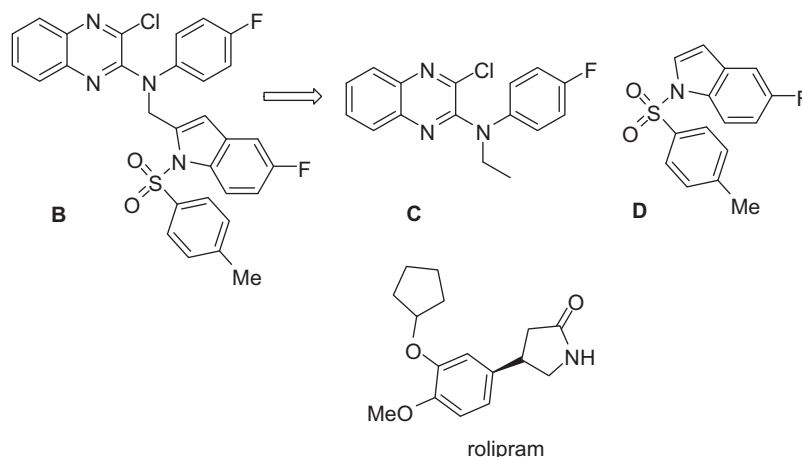


Figure 3 The specific molecule **B**, its two individual fragments **C** and **D** and the known PDE4 inhibitor rolipram.

Table 1 The dock score and summary of molecular interactions of top-ranked docking poses of **B**, **C** and **D** along with rolipram.

Compounds	MOE Dock score (kcal/mol)		H-bond interactions PDE4B
	PDE4B		
Rolipram	-24.61		His234, Gln443
B	-21.54		His 234
C	-15.29		Tyr233
D	-16.36		Tyr233

The optimized reaction condition for the synthesis of **6** was established by reacting the alkyne **4a** (Ar = C₆H₄Cl-*p*) with *N*-(2-iodophenyl)methanesulfonamide (**5a**) in the presence of 10% Pd/C–PPh₃–CuI as a catalyst system under various conditions (Table 2). The reaction afforded the expected product **6a** in 43% yield when performed in MeOH at 60 °C for 4 h (entry 1, Table 2). However, the product yield was increased to 78%

when the reaction was carried out in EtOH at 70 °C (entry 2, Table 2). We then assessed the role of catalyst, co-catalyst, ligand and base in the present reaction. The reaction afforded either poor yield of product **6a** or no product when performed in the absence of Pd/C (entry 3, Table 2), or CuI (entry 4, Table 2) or PPh₃ (entry 5, Table 2). All these reactions were performed using Et₃N as a base. However, the use of K₂CO₃ in place of Et₃N (entry 6, Table 2) was found to be less effective. A side reaction perhaps due to the reaction of **4a** with EtOH in the presence of K₂CO₃ was observed in this case. Thus the condition of entry 2 of Table 2 was used for the generation of a small library of molecules based on **A** (Chart 1). It is evident from Chart 1 that reactions proceeded well in all the cases to afford the desired product **6a-i** in good to acceptable yields. Compounds containing *N*-mesyl indole e.g. **6a-f** and *N*-tosyl indole moiety e.g. **6g-i** were synthesized conveniently using this strategy. It is worthy to mention that while chloro group of 3-chloroquinoxalin-2-amines is known to participate in the Pd/C–Cu mediated alkynylation reaction (Prasad et al.,

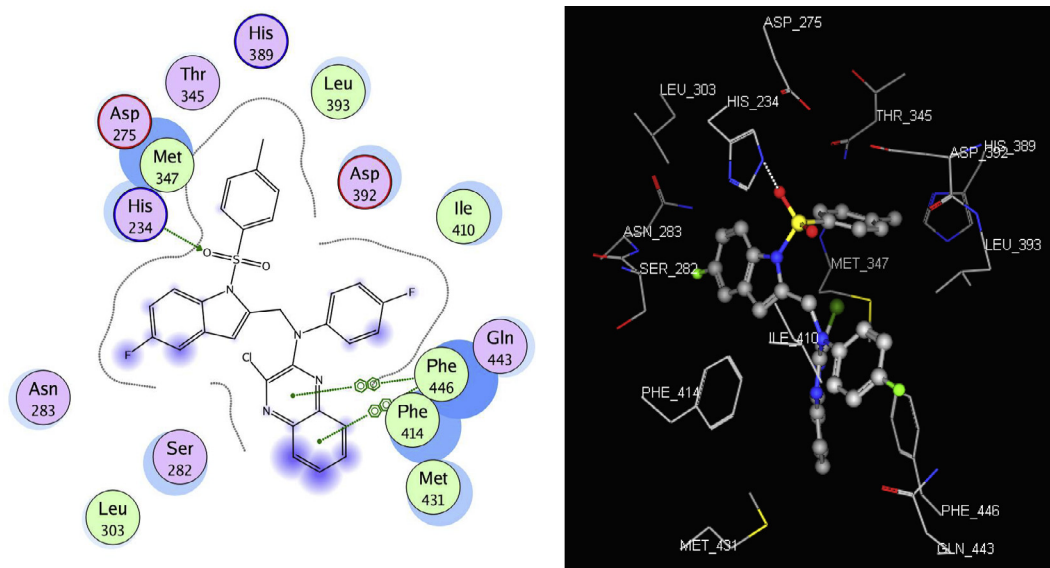
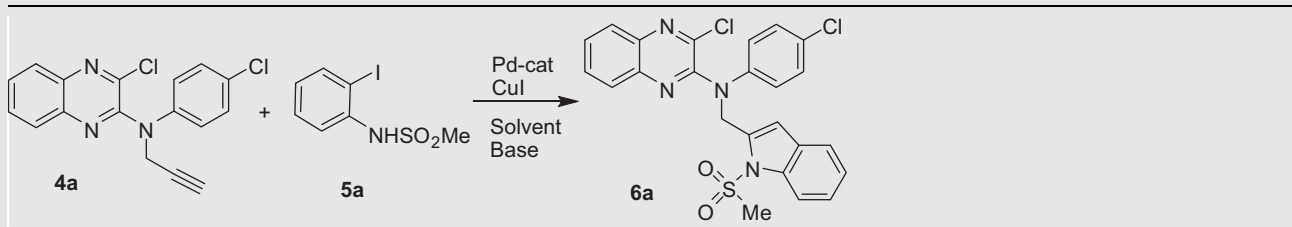


Figure 4 Docking of compound **B** into PDE4B (PDB code-1XMY).

Table 2 Effect of reaction conditions on coupling of terminal alkyne **4a** with *o*-iodoanilide **5a**.^a


Entry	Catalyst	Solvent/base	Temp (°C)/time (h)	% yield ^b
1	10%Pd/C-PPh ₃	MeOH/Et ₃ N	60/4	43
2	10%Pd/C-PPh ₃	EtOH/Et ₃ N	70/4	78
3	PPh ₃	EtOH/Et ₃ N	70/12	17 ^c
4	10%Pd/C-PPh ₃	EtOH/Et ₃ N	70/12	No product ^d
5	10%Pd/C	EtOH/Et ₃ N	70/12	10 ^e
6	10%Pd/C-PPh ₃	EtOH/K ₂ CO ₃	70/4	21

^a All reactions were carried out using **5a** (1 equiv.), alkyne **4** (1 equiv.), a Pd-catalyst (0.016 equiv.), PPh₃ (0.125 equiv.), CuI (0.02 equiv.), and a base (2 equiv.) in EtOH (5.0 mL), at 70 °C.

^b Isolated yield.

^c The reaction was carried out without Pd/C.

^d The reaction was carried out without CuI.

^e The reaction was carried out without PPh₃.

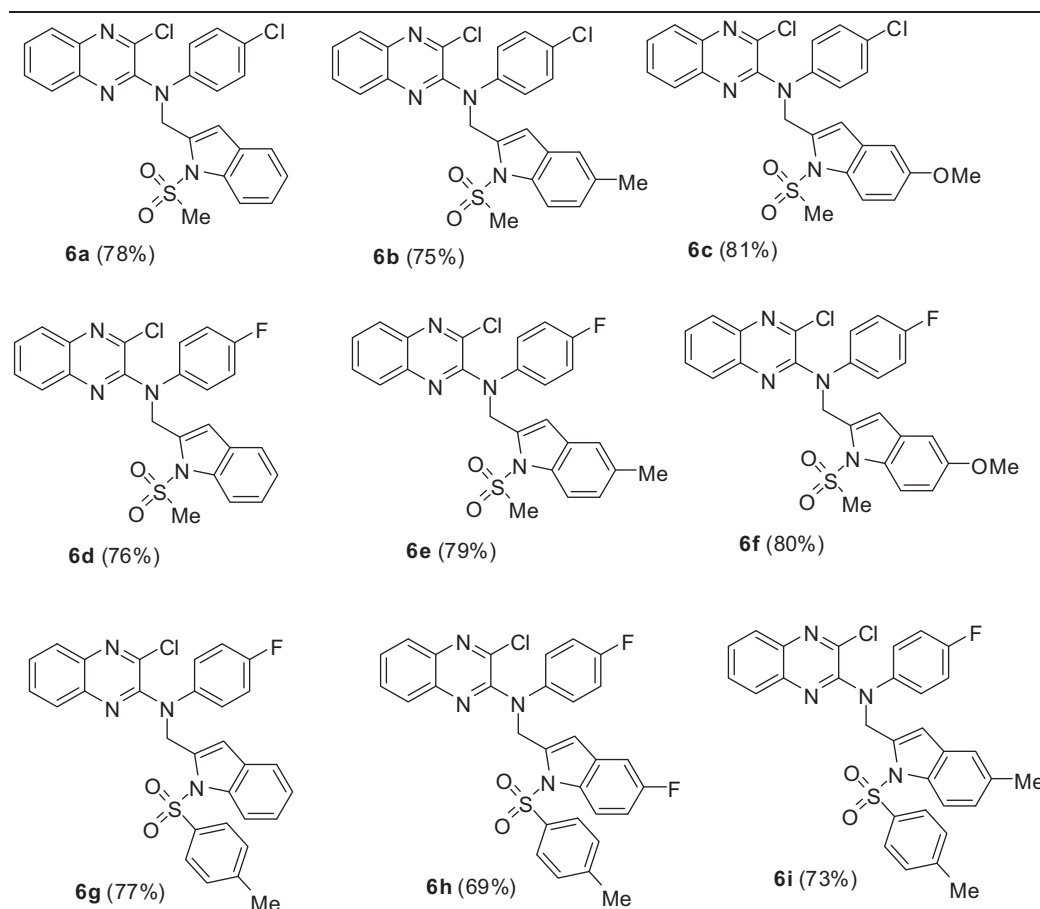


Chart 1 The list of quinoxaline-indole based hybrid molecules **6** prepared via Pd/C—Cu catalyzed coupling-cyclization strategy (Scheme 1). (All the reactions were carried out using alkyne **4** (1 equiv.), **5** (1 equiv.), 10% Pd/C (0.016 equiv.), PPh₃ (0.125 equiv.), CuI (0.02 equiv.), and Et₃N (2 equiv.) in EtOH at 70 °C for 4 h. Figures within the bracket indicate isolated yields.)

2012), the chloro group of **4** remained inert in the present reaction perhaps due to the higher reactivity of iodo group of **5** toward the Pd catalyst. Thus, the active Pd(0) species generated *in situ* (Pal, 2009; Pal et al., 2004; Layek et al., 2009) (Scheme 2) undergoes oxidative addition with **5** rather than **4** to give the organo-Pd(II) species **E-1** which on transorganometallation with copper acetylide generated *in situ* from CuI and **4** affords **E-2**. The reductive elimination of Pd(0) from **E-2** affords the internal alkyne **E-3** which subsequently undergoes Cu-mediated intramolecular ring closure to give the desired product **6** via **E-4**. Thus the whole process seemed to proceed via two catalytic cycles i.e. the Pd-cycle followed by a Cu-cycle.

All the quinoxaline-indole based hybrid molecules **6** prepared were characterized by spectral data and the selected ^1H and ^{13}C signals of a representative compound **6a** are shown in Fig. 5. Thus appearance of peaks at δ 6.79, 5.66 and 3.29 ppm in ^1H NMR spectra of **6a** was due to the C-3 indolyl proton, methylene group at C-2 of the indole ring and methyl group of mesyl moiety. The ^{13}C signals of compound **6a** observed at 148.9 and 142.2 ppm were due to the C-2 and C-3 carbon of the quinoxaline ring, and the signals at 139.7 and 109.9 ppm were due to the C-2 and C-3 carbon of indole ring. The other signals appeared at 145.6 ppm were due to the C-1 carbon of the 4-chlorophenyl ring, at 51.9 ppm were due to the methylene carbon and at 40.9 ppm were due to the mesyl carbon.

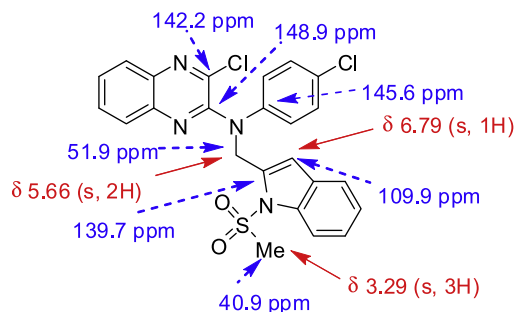
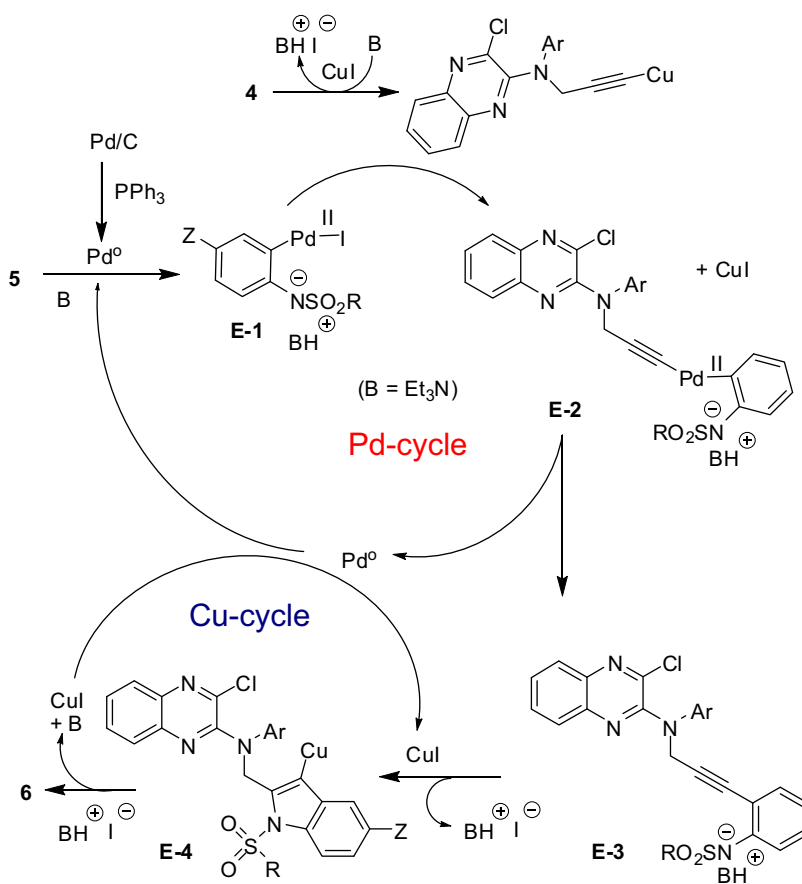


Figure 5 Selected ^1H and ^{13}C signals shown by compound **6a**.

3.3. Pharmacology

All the synthesized compounds were evaluated for their PDE4 inhibitory potential *in vitro* (Wang et al., 1997). While most of the compounds showed mediocre to good inhibition of PDE4B when tested at 30 μM the most notable were identified as **6a** (56% inhibition), **6e** (61%), **6g** (67%), **6h** (79%) and **6i** (64%). These compounds showed > 50% inhibition of PDE4B except **6h** that showed \sim 79% inhibition. The reference compound rolipram showed 90% inhibition at 10 μM in the same assay. While the docking of **6a** and **6e** into PDE4B showed good interactions with this protein (see supporting info) their dock score (-19.34 kcal/mol for **6a** and -19.70 kcal/mol for **6e**) indicated that **6h** (dock score -21.54 kcal/mol) interacted



Scheme 2 Proposed reaction mechanism for the Pd/C–Cu mediated coupling-cyclization **5** with **4** leading to the desired product **6**.

Table 3 Inhibition of PDE4B by compound **6h** and rolipram.

Compounds	% inhibition of PDE4B ^a				
	30 μ M	10 μ M	5 μ M	1 μ M	0.1 μ M
6h	79	63	48	31	ND
Rolipram	ND	90	73	53	32

ND = not determined.

^a Average of three determinations.

better. This is in agreement with the observed superior *in vitro* activities of compound **6h** (79% inhibition) compared to **6a** (56% inhibition) and **6e** (61% inhibition). Moreover, compounds **C** [prepared via AlCl₃ mediated reaction of **1** with *N*-ethyl-4-fluoroaniline (*cf* first step of Scheme 1)] and **D** (prepared via the reaction of 5-fluoroindole and *p*-tosyl chloride) were tested for their PDE4 inhibitory potential *in vitro*. As predicted earlier, both of these compounds (< 50% inhibition at 30 μ M) were found to be inferior compared to **6h** (i.e. **B**, Fig. 3). Overall, based on *in vitro* data the *N*-(*p*-tosyl) derivatives (**6g–i**) in general were identified as better inhibitors than the *N*-mesyl derivatives (**6a–f**). Among the *N*-(*p*-tosyl) derivatives, the presence of fluorine at C-5 position of the indole ring (e.g. **6h**) was beneficial over a hydrogen (e.g. **6g**) or methyl substituent (e.g. **6i**) at the same position. To assess the potential of compound **6h** further this compound was tested at different concentrations and the % inhibition observed is summarized in Table 3. The compound **6h** showed consistent dose-dependent inhibition of PDE4B across all the concentration tested and its IC₅₀ was calculated as 5.11 \pm 0.24 μ M. Moreover, this compound showed some selectivity toward PDE4B over PDE4D (e.g. 79% inhibition of PDE4B vs 41% inhibition of PDE4D at 30 μ M). Thus the compound **6h** was identified as a PDE4 inhibitor of further interest.

4. Conclusions

In conclusion, the concept of hybrid molecules has been explored as a new strategy to identify novel inhibitors of PDE4. Thus, a series of hybrid molecules were designed rationally by connecting an indole moiety with a quinoxaline ring through a linker as potential inhibitors of PDE4. Their design was validated initially *in silico* by performing docking studies using a representative molecule along with its two individual fragments. The combined form showed better results than the individual fragments. Subsequent synthesis of a focused library of related hybrid molecules was accomplished using a 3-step method, the Pd/C–Cu mediated coupling-cyclization being the key step. A range of compounds was synthesized in good yields some of which showed PDE4 inhibition *in vitro* and one of them appeared to be promising. Overall, this research would be a new addition to the rapidly growing area of bioactive hybrid molecules.

Acknowledgments

The authors thank Dr. Kishore and his group for pharmacological assay and the management of Dr. Reddy's Institute of Life Sciences, Hyderabad, for continuous support and encouragement.

Appendix A. Supplementary material

Supplementary data associated with this article can be found, in the online version, at <http://dx.doi.org/10.1016/j.arabjc.2015.08.009>.

References

- Babu, P.V., Mukherjee, S., Deora, G.S., Chennubhotla, K.S., Mediseti, R., Yellanki, S., Kulkarni, P., Sripelly, S., Parsa, K.V.L., Chatti, K., Mukkanti, K., Pal, M., 2013. Ligand/PTC-free intramolecular Heck reaction: synthesis of pyrroloquinoxalines and their evaluation against PDE4/luciferase/oral cancer cell growth *in vitro* and zebrafish *in vivo*. *Org. Biomol. Chem.* 2013 (11), 6680–6685.
- Card, G.L., England, B.P., Suzuki, Y., Fong, D., Powell, B., Lee, B., Luu, C., Tabrizizad, M., Gillette, S., Ibrahim, P.N., Artis, D.R., Bollag, G., Milburn, M.V., Kim, S.-H., Schlessinger, J., Zhang, K. Y.J., 2004. Structural basis for the activity of drugs that inhibit phosphodiesterases. *Structure* 12, 2233–2247.
- Chauhan, S.S., Sharma, M., Chauhan, P.M.S., 2010. Trioxaquinones: hybrid molecules for the treatment of malaria. *Drug News Perspect.* 23, 632–646.
- Corbeil, C.R., Williams, C.I., Labute, P., 2012. Variability in docking success rates due to dataset preparation. *J. Comput.-aided Molecular Des.* 26, 775–786.
- DeSimone, R.W., Currie, K.S., Mitchell, S.A., Darrow, J.W., Pippin, D.A., 2004. Privileged structures: applications in drug discovery. *Comb. Chem. High Throughput Screening* 7, 473–493.
- Draheim, R., Egerland, U., Rundfeldt, C., 2004. Anti-inflammatory potential of the selective phosphodiesterase 4 inhibitor N-(3,5-dichloro-pyrid-4-yl)-[1-(4-fluorobenzyl)-5-hydroxy-indole-3-yl]-glyoxylic acid amide (AWD 12-281), in human cell preparations. *J. Pharmacol. Exp. Ther.* 308, 555–563.
- Dym, O., Xenarios, I., Ke, H., Colicelli, J., 2002. Molecular docking of competitive phosphodiesterase inhibitors. *Mol. Pharmacol.* 61, 20–25.
- Evans, B.E., Rittle, K.E., Bock, M.G., DiPardo, R.M., Freidinger, R. M., Whitter, W.L., Lundell, G.F., Veber, D.F., Anderson, P.S., 1988. Methods for drug discovery: development of potent, selective, orally effective cholecystokinin antagonists. *J. Med. Chem.* 12, 2235–2246.
- França, T.C.C., Guimarães, A.P., Cortopassi, W.A., Oliveira, A.A., Ramalho, T.C., 2013. Applications of docking and molecular dynamic studies on the search for new drugs against the biological warfare agents *Bacillus anthracis* and *Yersinia pestis*. *Curr. Comput. Aided Drug Des.* 9, 507–517.
- Gangwal, R.P., Damre, M.V., Das, N.R., Dhoke, G.V., Bhadauriya, A., Varikoti, R.A., Sharma, S.S., Sangamwa, A.T., 2015. Structure based virtual screening to identify selective phosphodiesterase 4B inhibitors. *J. Mol. Graph. Model.* 57, 89–98.
- Gutke, H.J., Guse, J.H., Khobzaoui, M., Renukappa-Gutke, T., Burnet, M., 2005. AWD-12-281 (inhaled) (elbion/GlaxoSmithKline). *Curr. Opin. Investig. Drugs* 6, 1149–1158.
- Kodimuthali, A., Jabar, S.S.L., Pal, M., 2008. Recent advances on phosphodiesterase 4 inhibitors for the treatment of asthma and chronic obstructive pulmonary disease. *J. Med. Chem.* 18, 5471–5489.
- Kolli, S.K., Nakhi, A., Medishetti, R., Yellanki, S., Kulkarni, P., Raju, R.R., Pal, M., 2014a. NaSH in the construction of thiophene ring fused with *N*-heterocycles: a rapid and inexpensive synthesis of novel small molecules as potential inducers of apoptosis. *Bioorg. Med. Chem. Lett.* 24, 4460–4465.
- Kolli, S.K., Nakhi, A., Archana, S., Saridena, M., Deora, G.S., Yellanki, S., Mediseti, R., Kulkarni, P., Raju, R.R., Pal, M., 2014b. Ligand-free Pd-catalyzed C-N cross-coupling/cyclization strategy: an unprecedented access to 1-thienyl pyrroloquinoxalines

- for the new approach towards apoptosis. *Eur. J. Med. Chem.* 86, 270–278.
- Kumar, K.S., Rambabu, D., Sandra, S., Kapavarapu, R., Krishna, G. R., Rao, M.V.B., Chatti, K., Reddy, C.M., Misra, P., Pal, M., 2012a. AlCl_3 induced (hetero)arylation of 2,3-dichloroquinoxaline: a one-pot synthesis of mono/disubstituted quinoxalines as potential antitubercular agents. *Bioorg. Med. Chem.* 20, 1711–1722.
- Kumar, K.S., Rambabu, D., Prasad, B., Mujahid, M., Krishna, G.R., Rao, M.V.B., Reddy, C.M., Vanaja, G.R., Kalle, A.M., Pal, M., 2012b. A new approach to construct fused 2-ylidene chromene ring: highly regioselective synthesis of novel chromeno quinoxalines. *Org. Biomol. Chem.* 10, 4774–4781.
- Layek, M., Lakshmi, U., Kalita, D., Barange, D.K., Islam, A., Mikkanti, K., Pal, M., 2009. Pd/C-Mediated synthesis of indoles in water. *Beilstein J. Org. Chem.* 5. <http://dx.doi.org/10.3762/bjoc.5.46>.
- Lipworth, B.J., 2005. Phosphodiesterase-4 inhibitors for asthma and chronic obstructive pulmonary disease. *Lancet* 365, 167–175.
- McCall, J.M., John, R., Donnal, L., Clair, M. WO 2011028947 A2 20110310 PCT Int Appl., 2011.
- Nakhi, A., Archana, S., Seerapu, G.P.K., Chennubhotla, K.S., Kumar, K.L., Kulkarni, P., Haldar, D., Pal, M., 2013a. AlCl_3 -mediated hydroarylation/heteroarylation in a single pot: a direct access to densely functionalized olefins of pharmacological interest. *Chem. Commun.* 49, 6268–6270.
- Nakhi, A., Rahman, Md.S., Seerapu, G.P.K., Banote, R.K., Kumar, K.L., Kulkarni, P., Haldar, D., Pal, M., 2013b. Transition metal free hydrolysis/cyclization strategy in a single pot: synthesis of fused furo *N*-heterocycles of pharmacological interest. *Org. Biomol. Chem.* 11, 4930–4934.
- Oliveira, F.G., Sant'Anna, C.M.R., Caffarena, E.R., Dardenne, L.E., Barreiro, E.J., 2006. Molecular docking study and development of an empirical binding free energy model for phosphodiesterase 4 inhibitors. *Bioorg. Med. Chem.* 14, 6001–6011.
- Pal, M., 2009. Palladium-catalyzed alkylation of aryl and heteroaryl halides: a journey from conventional palladium complexes or salts to palladium/carbon. *Synlett*, 2896–2912.
- Pal, M., Venkataraman, S., Batchu, V.R., Dager, I., 2004. Synthesis of 2-substituted indoles via Pd/C catalyzed reaction in water. *Synlett*, 1965–1969.
- Prasad, B., Kumar, K.S., Babu, P.V., Anusha, K., Rambabu, D., Kandale, A., Vanaja, G.R., Kalle, A.M., Pal, M., 2012. AlCl_3 induced C–N bond formation followed by Pd/C–Cu mediated coupling-cyclization strategy: synthesis of pyrrolo[2,3-*b*]quinoxalines as anticancer agents. *Tetrahedron Lett.* 53, 6059–6059.
- Rabe, K.F., 2011. Update on roflumilast, a phosphodiesterase 4 inhibitor for the treatment of chronic obstructive pulmonary disease. *Br. J. Pharmacol.* 163, 53–67.
- Ramalho, T.C., Rocha, M.V.J., da Cunha, E.F.F., Freitas, M.P., 2009. The search for new COX-2 inhibitors: a review of 2002–2008 patents. *Expert Opin. Ther. Pat.* 19, 1193–1228.
- Spina, D., 2008. PDE4 inhibitors: current status. *Br. J. Pharmacol.* 155, 308–315.
- Sunke, R., Babu, P.V., Yellanki, S., Medishetti, R., Kulkarni, P., Pal, M., 2014. Ligand free MCR for linking quinoxaline framework with benzimidazole nucleus: a new strategy for the identification of novel hybrid molecules as potential inducers of apoptosis. *Org. Biomol. Chem.* 12, 6800–6805.
- Tralau-Stewart, C.J., Williamson, R.A., Nials, A.T., Gascoigne, M., Dawson, J., Hart, G.J., Angell, A.D.R., Solanke, Y.E., Lucas, F.S., Wiseman, J., Ward, P., Ranshaw, Lisa E., Knowles, R.G., 2011. GSK256066, an exceptionally high-affinity and selective inhibitor of phosphodiesterase 4 suitable for administration by inhalation: in vitro, kinetic, and in vivo characterization. *J. Pharmacol. Exp. Ther.* 337, 145–154.
- Wang, P., Myers, J.G., Wu, P., Cheewatrakoolpong, B., Egan, R.W., Billah, M.M., 1997. Expression, purification, and characterization of human cAMP-specific phosphodiesterase (PDE4) subtypes A, B, C, and D. *Biochem. Biophys. Res. Commun.* 234, 320–324.
- Welsch, M.E., Snyder, S.A., Stockwell, B.R., 2010. Privileged scaffolds for library design and drug discovery. *Curr. Opin. Chem. Biol.* 3, 347–361.